

IEEE 802.11p Performance for Vehicle-to-Anything Connectivity in Urban Interference Channels

Thomas Blazek¹, Golsa Ghiaasi², Christian Backfrieder³, Gerald Ostermayer³, Christoph F. Mecklenbräuer¹,

¹Institute of Telecommunications, TU Wien, Vienna, Austria, {tblazek,cfm}@nt.tuwien.ac.at

²Department of Electronics, NTNU, Trondheim, Norway, golsa.ghiaasi@ntnu.no

³Research Group Networks and Mobility, FH Upper Austria, Hagenberg, Austria, {christian.backfrieder,gerald.ostermayer}@fh-hagenberg.at

Abstract—All too often, the performance of vehicular communications is benchmarked for a single link only. A major challenge for performance benchmarking of multiple interacting vehicles is the definition of repeatable vehicular scenarios. In this paper, we propose and discuss an approach for performance analysis of the IEEE 802.11p standard in urban interference channels, by linking network simulations with a Software Defined Radio (SDR) setup. This approach provides communication performance measurements in the worst-case interference scenario caused by an urban traffic jam. We do this by starting out with vehicular traffic flow simulations and continue to model the medium access. We furthermore introduce an algorithm to reduce the complexity of the communication network while retaining its properties. Finally, we use a setup of SDRs encompassing of communication nodes and channel emulators that emulate urban channels to measure the packet level performance as a function of Signal-to-Interference Ratio (SIR) and distance to receiver under urban traffic conditions.

Index Terms—Intelligent Transport Systems, Interference, Urban Channel

I. INTRODUCTION

IEEE 802.11p [1] is the first established ad-hoc standard for Vehicle-to-Anything (V2X) communications. However, its default Medium Access Control (MAC) scheme, which is based on Carrier Sense Multiple Access with Collision Avoidance (CSMA/CA), combined with the need for frequent signaling of safety-relevant messages, has been contested on its scalability [2]. Furthermore, the ad-hoc nature leads to *hidden nodes* [3], resulting in interference at receivers. The urban scenario is interesting in this case, as it is characterized by small distances between vehicles due to low speeds involved, as well as the strong geometric localization of the vehicles. Hence, scalability and the performance of IEEE 802.11p has been a hot topic in research for the past years [4], [5]. Alternative channel access schemes were investigated [6] and the influence of hidden nodes was treated [7]. Most research however takes a pure system level approach, where the analysis is based on simulations and the influence of the physical channel is neglected. On the other hand, the vehicular physical channel has also been the center of analysis [8], [9]. There, on the other hand, a single link is considered, and the behavior under the existence of interference is not demonstrated. Some advances in the analysis of interference in vehicular communications have been made, but they are either theoretic or simulation

works [10], [11], or do not consider large scale networks, and focus on the interference between two nodes instead [12].

A. Our Contribution

The main contribution of this paper is the combination of large-scale vehicular network simulations with a hardware setup to provide in-lab measured results on the influence of interference in urban scenarios. We use OpenStreetMap [13] to obtain real-world street and building layouts of the city of Linz in Austria, and employ vehicular driving simulations [14] which provide us with real-life traffic scenarios. First, we use the MAC properties of IEEE 802.11p to describe and simulate the packet transmission and medium access under the assumption that all vehicles in the simulation are equipped with ad-hoc communication means, and simulate message propagation and collision in an ad-hoc network. Then, we approximate this behavior through a graph representation in a way that allows us to represent transmission using a small number of devices. Finally, we use the simulated results to measure the performance of IEEE 802.11p on Software Defined Radios (SDRs) that act as transmitters, interferers, receivers and channel emulators. We use channel emulators with vehicular channel models, and analyze the Packet Error Rate (PER), interferer number, Signal-to-Interference Ratio (SIR) and distance to receiver. This provides us with a realistic performance estimate of IEEE 802.11p in the challenging urban interference channels.

II. SYSTEM MODEL

We consider the scenario shown in Figure 1. A large number of vehicles are incoming from the north via two main streets and try to cross a bridge in the city of Linz in Austria. These vehicles are assumed to be equipped with IEEE 802.11p compliant hardware, and are thus able to communicate. The vehicles transmit safety beacon information of varying payload size at 5.9GHz using a rate of 10 packets per second. We model both pathloss and small-scale fading for single link communications, as well as the Physical Layer (PHY) and MAC scheme for IEEE 802.11p. Since we have map data for the region of interest, we are able to distinguish Line-of-Sight (LOS) and Non Line-of-Sight (NLOS) from this data.

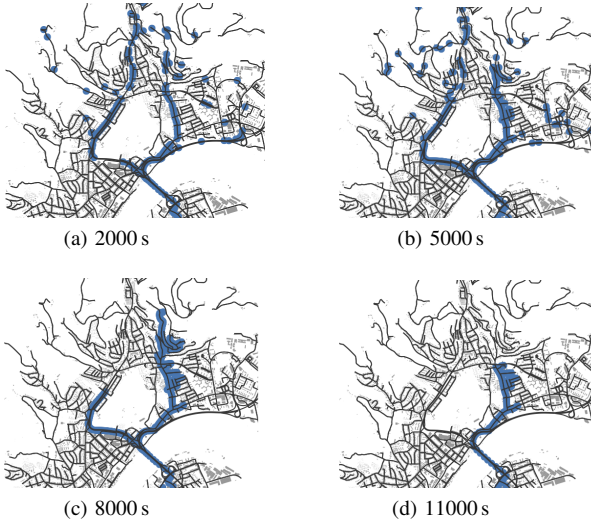


Fig. 1. Four snapshots at different simulation times of the traffic flow simulation.

A. Physical and Medium Access Control

We assume the PHY layer as defined by the 802.11p standard, which uses Orthogonal Frequency Division Multiplexing (OFDM) at 5.9 GHz at a bandwidth of 10 MHz [1]. We choose 10 dBm as transmit power for our communication nodes. IEEE 802.11p uses CSMA/CA as MAC scheme. Therefore, a node only transmits when it perceives the channel to be empty. This is done by measuring the Received Signal Strength Indicator (RSSI), and comparing it to a threshold. We chose this threshold to be -80 dBm, resulting in *sensing range* of 323 m. Whenever two vehicles are within this sensing range of each other, they will not transmit simultaneously.

B. Pathloss and Fading

Karedal et al. proposed an empirical pathloss model for urban scenarios in [15] as

$$PL_0 = 20 \log_{10} \frac{4\pi f_0}{c_0}$$

$$P(d) = PL_0 + 16.8 \log_{10}(d/1m) + X_{\sigma_2} + \zeta PL_c, \quad (1)$$

Where $f_0 = 5.9$ GHz, c_0 is the speed of light, X_{σ_2} is a lognormal model for shadowing, and ζ and PL_c account for stochastic shadowing. Using the map data, we can show that around the point of most interference, there are no large-scale obstructions, as it is surrounded by water on one side, and a large field on the other, and therefore we neglect the corresponding terms by setting X_{σ_2} and ζ to 0.

We account for small-scale fading using a tapped-delay line based channel emulator [16], hence we use the delay line fading model which results in the time-variant impulse response

$$\mathcal{H}(t, \tau) = \sum_{i=1}^N \eta_i h_i(t) \delta(\tau - \tau_i), \quad (2)$$

TABLE I
URBAN LOS DELAY LINE [17]

Tap	η_i^2 [dB]	τ_i [ns]	$f_{i,d}$ [Hz]	Profile
$i = 1$	0	0	0	Static
$i = 2$	-8	117	236	HalfBT
$i = 3$	-10	183	-157	HalfBT
$i = 4$	-15	333	492	HalfBT

where the parameters are set according to [17]. Specifically, we use a channel model defined for IEEE 802.11p, which uses 4 taps, and asymmetric half-bathtub shaped Doppler spectra. Since we do not assume shadowing, we use the *Urban LOS* model, for which the channel parameters are shown in Table I.

III. NETWORK MODELING

In this section, we present our model of the packet transmission network. First, we introduce the traffic flow simulations on which our analysis is based. In a second step, we use the chosen PHY and MAC parameters to define a communication network, based on the relative vehicle positions obtained from the traffic simulations. From this we define a communication graph. Finally, we impose simplifications on the communication graph that allow us to represent the graph using a small number of physical nodes. Based on those simplifications, we present an algorithm that approximates the original communication graph, while fulfilling the given restrictions.

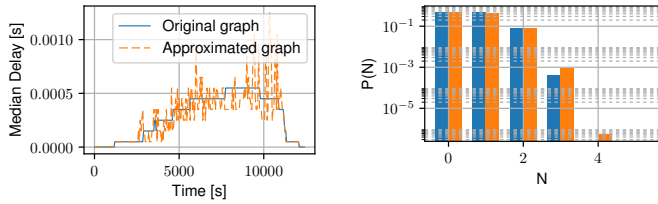
A. Traffic Simulations

The simulations are conducted using the microscopic traffic simulator TraffSim [18]. The simulation setup presented in [14] consists of an excerpt of the city of Linz, with data gathered from OpenStreetMap. The simulation generates 3000 vehicles, whose start and end points are chosen at random in certain areas of the map, corresponding to commuter traffic from the northern side of the river to the southern side. As longitudinal model, the Intelligent Driver Model (IDM) is applied, and no coordination between the vehicles with respect to their routing is allowed. Figure 1 displays 4 snapshots at different simulation times. The bridge over the stream poses a unique bottleneck, especially with two main roads merging that are both undergoing a traffic jam.

All vehicles are expected to communicate according to the parameters described in Section II. The chosen MAC scheme distinguishes vehicles that *sense* a transmitter, i.e. vehicles whose received power is above a given threshold, even if the transmitted packet is not successfully decoded, from the others. For all vehicles that do sense each other, there will be no simultaneous transmissions. Hence, we introduce a communication graph

$$G = (V, E) \quad (3)$$

that consists of the node set V that contains all vehicles v_i , and the edge set E that contains all edges $e(i, j)$ where the nodes v_i and v_j are within sensing range of each other [19].



(a) Median channel access delay. (b) Probability of N incoming packets.

Fig. 2. Graph approximation evaluation.

On this graph, we simulate the safety beaconing according to the standard settings for safety relevant messages [20], Access Class (AC) 3. Each node transmits 10 packets per second, if two nodes that share an edge transmit simultaneously, they will choose a random backoff according to the standard and retransmit. After 7 failed transmission attempts, the message is discarded.

B. Network Approximation

Our goal is to represent the given scenario with a small number of hardware devices, however the shape of the communication graph G prohibits such an approach. To this end, we consider *cliques*, which are subsets $C \subset V$ of the node set where all nodes are connected with all others via edges, i.e. $e(i, j) \in E \forall v_i, v_j \in C$. In such a clique, it is guaranteed that only one node transmits at any given time. If, furthermore no node of the clique is connected to a node outside the clique, then the timing of the messages can be fully simulated within a given clique. Then, such a clique can be represented by just 1 transmitter.

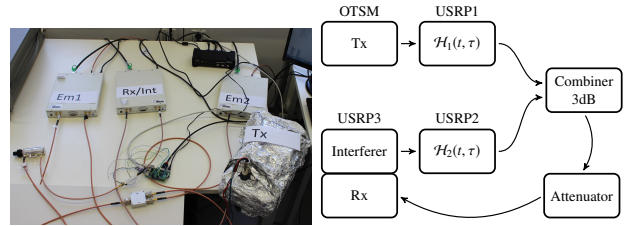
Hence, we devised Algorithm 1, which takes the original graph G as input, and approximates it with a graph that consists purely of cliques, which are not connected. As seed for the algorithm, we find all cliques of maximal size (a clique is of maximal size if no node $v_i \in V \setminus C$ can be added such that C remains a clique) [21]. These cliques may overlap however.

Algorithm 1 Clique Graph Approximation

```

1: procedure APPROXIMATED GRAPH(Graph  $G_O$ )
2:    $C \leftarrow \text{maxcliques}(G_O)$ 
3:   while Overlap between cliques exists do
4:     for all  $\{(i, j) \mid \text{OL}(C(i), C(j)) < t\}$  do
5:       remove overlap from  $C(i), C(j)$ 
6:     end for
7:     for all  $\{(i, j) \mid \text{OL}(C(i), C(j)) \geq t\}$  do
8:        $C(i) \leftarrow C(i) \cup C(j)$ 
9:        $C \leftarrow C \setminus C(j)$ 
10:    end for
11:  end while
12:  return Graph( $C$ )
13: end procedure

```



(a) Lab setup.

(b) Schematic of setup.

Fig. 3. Measurement setup.

Next, we calculate the Szymkiewicz-Simpson coefficient, also called overlap index [22]

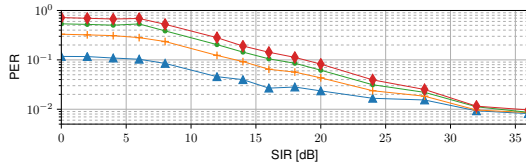
$$OL(\mathcal{A}, \mathcal{B}) = \frac{|\mathcal{A} \cap \mathcal{B}|}{\min(|\mathcal{A}|, |\mathcal{B}|)}, \quad (4)$$

which measures how much of the smaller of two sets is also contained in the larger one. We compare this overlap index to a threshold, and for all pairs below the threshold, chosen to be $t = 0.7$, we remove the overlap from the smaller clique (line 5). For all pairs with a larger overlap, the cliques are merged into a larger clique, and the smaller clique is removed from the set of cliques. In this way, strongly overlapping cliques are gradually merged, and cliques with little overlap are separated, until the graph consists purely of disjoint cliques.

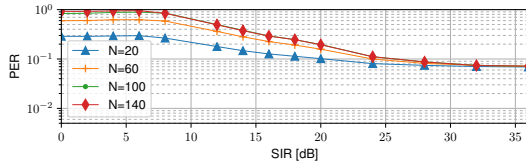
To assess the performance of this algorithm, we are interested if the packet transmission statistics between the original graph and the approximated graph are comparable. We simulate the median channel access delay (Figure 2a), as well as the probability of a node seeing N parallel incoming transmissions (Figure 2b). The results show 2 noteworthy properties. The median statistics captures the original well apart from noise introduced due to this quantization. Therefore, the approximated clique graph can be used as a graph with similar behavior. Furthermore, both pose strongly similar collision probabilities. Finally, almost the full probability in both cases is concentrated in $N \in [0, 2]$, meaning that a node almost never sees more than 2 simultaneous incoming packets. Therefore, we argue that 2 transmitters can be used to effectively emulate the behavior of a larger number of vehicles.

IV. INTERFERENCE MEASUREMENTS

Figure 3 shows a photo and schematic of the employed measurement setup. We use one Off-the-Shelf Modem (OTSM) as a transmitter that transmits 500000 packets in a continuous stream for every measurement point. As a second transmitter, we use a National Instruments (NI) Universal Software Radio Peripheral (USRP)-2953R SDR, that is controlled via the 802.11 application framework modified for 11p. This second transmitter acts as interferer, since we can transmit arbitrarily scheduled packets of any length through the use of a User Datagram Protocol (UDP) socket. As source, we take the packet level simulations of a clique, and transmit the resulting packet trace with the corresponding timings. Both transmitters are fed through channel emulators, which



(a) 258 Bytes



(b) 500 Bytes

Fig. 4. PER over SIR for interfering cliques of different sizes. For 500 bytes, no difference exists for 100 and 140 interferers.

are also implemented on Universal Software Radio Peripheral with Reconfigurable I/Os (USRP RIOs). Since the interferer represents multiple nodes that will see different pathlosses, the channel emulator in the interferer path additionally can switch path gain on a per millisecond basis to emulate this behavior. Afterwards, both paths are combined in a power combiner, and passed through a final RADITEK RVATTN-DC-6 (0-70 dB) switched attenuator back to the receiver path of the USRP. Our focus is the achieved performance in terms of PER, which is largely influenced by the SIR.

A. SIR Dependence

We first analyze the behavior of the PER in the presence of a single clique with constant pathloss and size. In this measurement, RSSI values of transmitter are set at -50 dB to simulate perfect conditions, and interferer are constant SIRs, which we define as the difference in decibels of the RSSIs, from 0 to 36 dB. We furthermore considered two different sizes for the packet transmissions (258 and 500 bytes), and we considered interfering clique sizes of 20, 60, 100 and 140 vehicles. Figure 4 shows the results of the measurements. In all cases, the PER remains constant up until a breakpoint of 6 dB. Above 30 dB, the interference is not noticeable anymore, and all scenarios approach their respective interference free performance.

B. Distance Dependence

In order to investigate distance dependence, we define fixed coordinates for the receiver position. This position, along with the sensing range, are shown in Figure 5. The coordinates are chosen such that the incoming roads are covered in the sensing range as evenly as possible. The figure furthermore depicts a snapshot of the vehicles, as well as the clique clustering that results from our approximation. We see the main cluster around the receiver, as well as 2 incoming clusters that act as interferer that do not sense each other. The number of vehicles in each clique for the full simulation duration can be seen in Figure 6a. Figure 6b shows the minimum and maximum

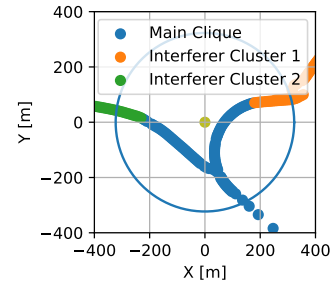
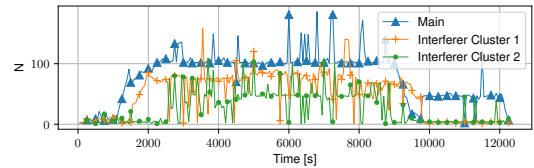
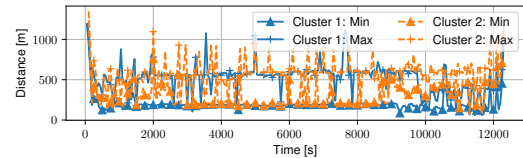


Fig. 5. Snapshot of clique distribution.



(a) Clique sizes.



(b) Clique distances.

Fig. 6. Change of clique parameters over simulation time.

Euclidean distances from the vehicles in each clique to the receiver. Figure 6 demonstrates that the traffic jam at the point of interest enters a stationary state at simulation time 2500 s, and continues until 9000 s. During that stationarity region, apart for random events, the cliques remain of constant size, and both interfering clusters stay at constant minimum and maximum ranges, which are furthermore almost identical for the two clusters. Hence, we concentrate on this stationarity region for our further measurements. To set the RSSI for the signal of interest, we evaluate Equation (1) for distances of 25, 50 and 100 m. To model the interference, we first generate packet transmissions for each of the 2 interfering cliques. Here, we use 2 configurations. The first configuration assumes one usable channel. The second configuration assumes traffic can be split into 3 dedicated channels, which is in accordance with the given standards [23]. Since the interfering vehicles are on a mostly straight street, we model pathloss by drawing a random distance uniformly between the minimum and maximum values, and set the pathloss accordingly. We overlay the transmissions from interfering cliques with equal distance distributions on one device. Our final simplification is that we draw a new distance every 1 ms. This does not ensure that the interfering pathloss only changes between transmissions, but we argue that this will not influence the results. The results are given in Figure 7. The results show that within the stationarity

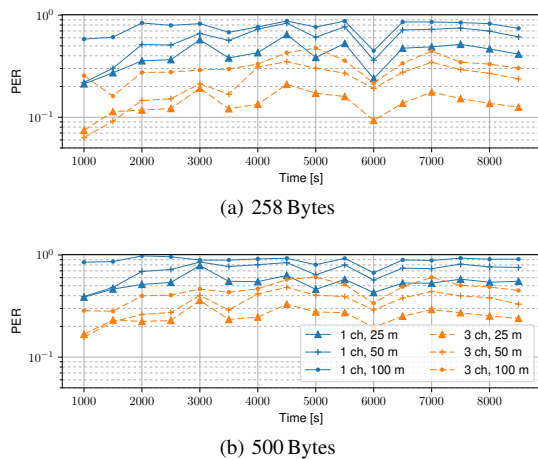


Fig. 7. PER simulation time for 1 and 3 used channels, and distances of 25, 50 and 100m to the receiver.

region the resulting PERs assume an almost constant value, with small fluctuations caused by the fluctuations of the clique sizes. Furthermore, we do have a uniformly high packet loss, with only short packets, close to the receiver seeing a small amount of throughput. The throughput can be improved by using short packets and 3 channels, however even then packet loss reaches more than 20% for a distance of 100m to the receiver.

V. CONCLUSIONS

We presented an approach to measuring the behavior of IEEE 802.11p under the influence of an urban interference channel. Our approach allows producing urban interference channel measurements in a lab setting using an equivalent scenario with a manageable amount of SDRs. We chose a scenario that is representative of the worst case that is encountered in urban communication scenarios, with severe traffic jams merging and no obstructions to reduce the interference. We confirm through measurements that without higher-layer control, IEEE 802.11p suffers severely in such a scenario. The use of multiple channels is required to allow communications, and algorithms like the Distributed Congestion Control (DCC) which control the transmit frequency, transmit power and receiver sensitivity are expected to ensure reception quality. Our results suggest that modifying these parameters is indeed required to achieve reliable packet delivery probabilities. The setup we presented here can be used to evaluate transmission parameters and test the resilience against interference in urban communication channels, and can contribute to finding a compromise between throughput and channel load.

REFERENCES

- [1] *Information technology—Telecommunications and information exchange between systems Local and metropolitan area networks—Specific requirements Part 11: Wireless LAN Medium Access Control (MAC) and Physical Layer (PHY) Specifications*, Std. ISO/IEC/IEEE 8802-11:2012(E) (Revision of ISO/IEC/IEEE 8802-11-2005 and Amendments), Nov 2012.
- [2] K. Sjöberg, E. Uhlemann, and E. Ström, “Scalability Issues of the MAC Methods STDMA and CSMA of IEEE 802.11p When Used in VANETs,” in *Int. Conf. Commun. Work.* IEEE, May 2010, pp. 1–5.
- [3] —, “How Severe Is the Hidden Terminal Problem in VANETs When Using CSMA and STDMA?” in *2011 Veh. Technol. Conf. (VTC Fall)*. IEEE, Sep 2011, pp. 1–5.
- [4] L. Stibor, Y. Zang, and H.-J. Reuerman, “Evaluation of Communication Distance of Broadcast Messages in a Vehicular Ad-Hoc Network Using IEEE 802.11p,” in *Wirel. Commun. Netw. Conf.* IEEE, 2007, pp. 254–257.
- [5] C. Han, M. Dianati, R. Tafazolli, R. Kernchen, and X. Shen, “Analytical Study of the IEEE 802.11p MAC Sublayer in Vehicular Networks,” *IEEE Trans. Intell. Transp. Syst.*, vol. 13, no. 2, pp. 873–886, Feb 2012.
- [6] X. Ma, X. Chen, P. Hightower, M. Abdul-hak, N. Al-Holou, U. Mohammad, K. Sjöberg, E. Uhlemann, E. Ström, A. M. S. Abdelgader, W. Lenan, S. M. Nazir, and R. Rastogi, “The Physical Layer of the IEEE 802.11p WAVE Communication Standard: The Specifications and Challenges,” *Electr. Veh. - Model. Simulations*, vol. II, no. 3, 2014.
- [7] Y. Zang, B. Walke, G. Hiertz, and C. Wietfeld, “IEEE 802.11p-based Packet Broadcast in Radio Channels with Hidden Stations and Congestion Control,” Dec 2016.
- [8] C. F. Mecklenbräuker, A. F. Molisch, J. Karedal, F. Tufvesson, A. Paier, L. Bernado, T. Zemen, O. Klemp, and N. Czink, “Vehicular Channel Characterization and Its Implications for Wireless System Design and Performance,” *Proc. IEEE*, vol. 99, no. 7, pp. 1189–1212, Jul 2011.
- [9] L. Bernado, T. Zemen, F. Tufvesson, A. F. Molisch, and C. F. Mecklenbräuker, “Delay and Doppler Spreads of Nonstationary Vehicular Channels for Safety-Relevant Scenarios,” *Trans. Veh. Technol.*, vol. 63, no. 1, pp. 82–93, Jan 2014.
- [10] P. Fazio, F. De Rango, C. Sottile, and C. Calafate, “A New Channel Assignment Scheme for Interference-Aware Routing in Vehicular Networks,” in *73rd Veh. Technol. Conf. (VTC Spring)*. IEEE, May 2011, pp. 1–5.
- [11] I. Khan and J. Harri, “Can IEEE 802.11p and Wi-Fi coexist in the 5.9GHz ITS band ?” in *18th Int. Symp. A World Wireless, Mob. Multimed. Networks.* IEEE, Jun 2017, pp. 1–6.
- [12] M. Fadda, M. Murrioni, and V. Popescu, “Interference Issues for VANET Communications in the TVWS in Urban Environments,” *Trans. Veh. Technol.*, vol. 65, no. 7, pp. 4952–4958, Jul 2016.
- [13] OpenStreetMap contributors, “Planet dump retrieved from <https://planet.osm.org>,” <https://www.openstreetmap.org>, 2017.
- [14] C. Backfrieder, G. Ostermayer, and C. F. Mecklenbräuker, “Increased Traffic Flow Through Node-Based Bottleneck Prediction and V2X Communication,” *Trans. Intell. Transp. Syst.*, vol. 18, no. 2, pp. 349–363, Feb 2017.
- [15] J. Karedal, N. Czink, A. Paier, F. Tufvesson, and A. F. Molisch, “Path Loss Modeling for Vehicle-to-Vehicle Communications,” *Trans. Veh. Technol.*, vol. 60, no. 1, pp. 323–328, Jan 2011.
- [16] G. Ghiaasi, M. Ashury, Z. Xu, D. Vlastaras, M. Hofer, and T. Zemen, “Real-Time Vehicular Channel Emulator for Future Conformance Tests of Wireless ITS Modems,” in *Proc. 10th Eur. Conf. Antennas Propag.*, Davos, 2016, pp. 1–5.
- [17] T. Blazek, C. Mecklenbräuker, D. Smely, G. Ghiaasi, and M. Ashury, “Vehicular channel models: A system level performance analysis of tapped delay line models,” in *15th International Conference on ITS Telecommunications*, May 2017.
- [18] C. Backfrieder, G. Ostermayer, and C. F. Mecklenbräuker, “TraffSim - A traffic simulator for investigations of congestion minimization through dynamic vehicle rerouting,” *International Journal of Simulation Systems, Science and Technology*, vol. 15, no. 4, pp. 38–47, Aug. 2014.
- [19] T. Blazek, C. Backfrieder, C. Mecklenbräuker, and G. Ostermayer, “Improving communication reliability in intelligent transport systems through cooperative driving,” in *10th IFIP Wireless and Mobile Networking Conference*, Sep. 2017.
- [20] S. Eichler, “Performance Evaluation of the IEEE 802.11p WAVE Communication Standard,” in *Veh. Technol. Conf.* IEEE, Sep 2007, pp. 2199–2203.
- [21] C. Lee, F. Reid, A. Mcdaid, and N. Hurley, “Detecting Highly Overlapping Community Structure by Greedy Clique Expansion,” 2010. [Online]. Available: <https://arxiv.org/abs/1002.1827v2>
- [22] S. Sharma and M. Singh, “Generalized similarity measure for categorical data clustering,” in *Int. Conf. Adv. Comput. Commun. Informatics*. IEEE, Sep 2016, pp. 765–769.
- [23] ETSI, “EN 302 663 - V1.2.0 - Intelligent Transport Systems (ITS); Access layer specification for Intelligent Transport Systems operating in the 5 GHz frequency band,” 2012.